Title

Paleointensity results from the Jurassic: New constraints from submarine basaltic glasses of ODP Site 801C

Journal

Geochemistry Geophysics Geosystems, 14(10)

ISSN

1525-2027

Authors

Tauxe, L
Gee, JS
Steiner, MB
et al.

Publication Date

2013-10-01

DOI

10.1002/ggge.20282

Peer reviewed

Geochemistry Geophysics Geosystems G3

Article
Volume 14, Number 10
29 October 2013
doi: 10.1002/ggge.20282
ISSN: 1525-2027

Published by AGU and the Geochemical Society

Paleointensity results from the Jurassic: New constraints from submarine basaltic glasses of ODP Site 801C

L. Tauxe and J. S. Gee
Geosciences Research Division, Scripps Institution of Oceanography, La Jolla, California, 92093-0220, USA (ltauxe@ucsd.edu)

M. B. Steiner
Department of Geology and Geophysics, University of Wyoming, Laramie, Wyoming, USA

H. Staudigel
Institute of Geophysics and Planetary Physics, Scripps Institution of Oceanography, La Jolla, California, USA

[1] Tholeiite of the oldest oceanic crust was drilled during ODP Legs 129 and 185 at Hole 801C in the western Pacific. Fresh appearing submarine basaltic glass (SBG) was recovered from the tholeiites (~167 Ma) which has been shown to be nearly ideal for determining absolute paleointensity. Paleointensities of the younger, off-axis, alkalic basalts (~160 Ma), overlying the tholeiites, had been studied earlier. Here we report results from the older tholeiitic (on-axis) sequence. We subjected a total of 73 specimens from 17 cooling units to absolute paleointensity experiments. Of these, 30 specimens and six cooling unit averages met our strictest reliability criteria, yielding an average of 11.9 ± 3.9 μT. The bulk of evidence suggests a paleolatitude of the site of 14°S (with an uncertainty of 10°). This translates the intensity to a value for the virtual axial dipole moment of 28 ZAm^2, slightly lower than values determined from the plagioclase crystals in the three cooling units of the younger alkalic basalts overlying the tholeiites (Tarduno & Cottrell, 2005). Our value is low when compared to the long-term median value of the field of 42 ZAm^2. Our results and those of the published literature therefore support the contention of a low magnetic field strength in the Jurassic (average of 28 ± 14 ZAm^2; $N = 138$ individual estimates), as initially suggested by Prévot et al. (1990). Our interpretation of the body of available data argue for low field strengths for the entire Jurassic extending into the early Cretaceous.

Components: 10,564 words, 7 figures, 4 tables.

Keywords: Mesozoic Dipole Low; Jurassic; paleointensity; paleomagnetism; submarine basaltic glass; ODP leg 185.

Index Terms: 1521 Paleointensity: Geomagnetism and Paleomagnetism; 1560 Time variations: secular and longer: Geomagnetism and Paleomagnetism; 1594 Instruments and techniques: Geomagnetism and Paleomagnetism; 1550 Spatial variations attributed to seafloor spreading: Geomagnetism and Paleomagnetism; 1599 General or miscellaneous: Geomagnetism and Paleomagnetism; 3005 Marine magnetics and paleomagnetics: Marine Geology and Geophysics.

Received 25 February 2013; **Revised** 30 September 2013; **Accepted** 1 October 2013; **Published** 29 October 2013.

Tauxe, L., J. S. Gee, M. B. Steiner, and H. Staudigel (2013), Paleointensity results from the Jurassic: New constraints from submarine basaltic glasses of ODP Site 801C, *Geochem. Geophys. Geosyst.*, *14*, 4718–4733, doi:10.1002/ggge.20282.

1. Introduction

[2] Despite numerous compilations of data on the strength of the geomagnetic field over time [e.g., *Tanaka et al*., 1995; *Perrin and Schnepp*, 2004; *Perrin and Shcherbakov*, 1997; *Tauxe and Yamazaki*, 2007; *Biggin*, 2010], fundamental properties of the field such as the average strength and its variation over time remain hotly debated. Most paleointensity data come from the last few hundred thousand years, and the data for characterizing field strength for the more distant past become increasingly sparse. As a result, there are competing views as to whether there was a period of unusually low geomagnetic field strength in the Jurassic and early Cretaceous, a period known as the "Mesozoic Dipole Low" (MDL) [*Prévot et al*., 1990]. Recently, champions for the existence of the MDL have sought to tie it to changes in whole mantle convection processes [e.g., *Tarduno and Cottrell*, 2005; *Biggin et al*., 2012]. However, there remains much debate in the literature on the related problems of what the long-term average value of the field is [*Juarez et al*., 1998; *Selkin and Tauxe*, 2000 versus *Biggin and Thomas*, 2003], and the duration [*Tarduno and Cottrell*, 2005 versus *Perrin and Shcherbakov*, 1997] or even existence [e.g., *Goguitchaitchvili et al*., 2002a versus *McElhinny and Sager*, 2003] of the MDL.

[3] Here we present new results from Jurassic aged submarine basaltic glass recovered from ODP Hole 801C, drilled in the western Pacific Ocean during Leg 185 and dated by *Koppers et al*. [2003] at ~167 Ma. For comparison, we compile the published paleointensity data from the Jurassic. In order to have a complete picture of the published data, we have included all results regardless of experimental design. In the process, we have updated age information and corrected the many mistakes in the PINT and MagIC database records.

2. The Mesozoic Dipole Low Controversy

2.1. The Jurassic Database

[4] *Cande et al*. [1978] first postulated the existence of a period of unusually low geomagnetic field strength combined with a rapid rate of polarity reversals for the oldest ocean crust. They observed a gradual increase in anomaly amplitude from at least as early as anomaly M29 extending to around M20 (158–146 Ma, according to the timescale of *Gradstein et al*. [2004]) which they argue explains the "Jurassic Quiet Zone" observed in marine magnetic anomalies in the western Pacific Ocean. This behavior is in stark contrast to the "Cretaceous Quiet Zone" which was thought to be a period with no polarity reversals spanning millions of years [*Helsley and Steiner*, 1969] possibly associated with high magnetic field intensities [*Tauxe and Staudigel*, 2004; *Tarduno and Cottrell*, 2005; *Tauxe and Yamazaki*, 2007].

[5] *Prévot et al*. [1990] compiled absolute paleointensity data for the Jurassic and early Cretaceous (Pliensbachian to Hauterivian or ~190–~130 Ma according to *Gradstein et al*. [2004] and estimated the average value to be ~32 ZAm^2. They tied the long period of low intensity to a minimum in "true polar wander" (TPW), thought by the authors to have occurred during the Jurassic. We note, however, that the higher rate of TPW during the Cretaceous called for by *Prévot et al*. [1990] subsequent to the MDL (attributed to *Courtillot and Besse* [1987]) was based on a "fixed hot spot model," which has been largely dismissed [*Tarduno and Gee*, 1995; *Tarduno and Smirnov*, 2001]. The older limit of the proposed MDL is not in contradiction with the data of *Cande et al*. [1978] whose anomaly record did not extend to times earlier than M29. A younger limit of early Cretaceous (M5–M11), however, is much younger than the prediction of *Cande et al*. [1978] who suggested that the field reached a stable, higher field value by M19 time. While *Tarduno and Cottrell* [2005] argued that low fields are restricted to times with high reversal frequencies, they relied on data from single crystal results which come from only three cooling units within Jurassic off-axis volcanism (~160 Ma) to support their argument. Clearly additional data would be helpful.

2.2. The Long-Term Average Intensity

[6] What constitutes a "low" field depends not only on the average field intensity during the period in question, but also on the "average" value against which it is compared. The latter was long thought to be close to the present day value (~80 ZAm^2). *McFadden and McElhinny* [1982] estimated the average for the last 5 Ma to be 86 ± 36 ZAm^2. It is interesting to note that while *Tanaka et al*. [1995] supported a near present day average field strength for the last 10 Ma of ~82 ZAm^2 in their paleointensity compilation, they questioned the reality of the MDL, pointing out that 90% of

the MDL data came from a single region, Armenia and its environs [*Bol'shakov and Solodovnikov*, 1980, 1983; *Bol'shakov et al*., 1987] and that one study thought to be Jurassic [*Derder et al*., 1989] had quite high field values.

[7] In a departure from the prevailing wisdom that held that the average geomagnetic field intensity was close to the present day value, *Juarez et al*. [1998] presented new data for the last 160 Myr from submarine basaltic glass (SBG) obtained by drilling the oceanic crust during expeditions by the Deep Sea Drilling Project (DSDP) and the Ocean Drilling Program (ODP) and argued for a lower average field value of ~42 ZAm^2 for the last 160 Myr. They commented that the Jurassic average of *Prévot et al*. [1990] was not "low" but may simply be average. A follow up paper by *Selkin and Tauxe* [2000] argued that the published data were heavily biased to more recent periods when the field does average to about the present dipole average of about 80 ZAm^2. To overcome the bias, they split the data into two time periods with roughly equal number of data points, those less than 0.3 Ma and those 0.3–300 Ma and estimated an average field of 84 ZAm^2 for the former and 46 ZAm^2 for the latter.

[8] *Thomas and Biggin* [2003] took issue with the data selection criteria used in the *Selkin and Tauxe* [2000] compilation of published data. In an attempt to compare data of similar quality, *Selkin and Tauxe* [2000] had excluded all data sets that were not done by double heating methods including pTRM checks (a widely used test for alteration). In fact, the exclusion of studies with no pTRM checks does indeed change the debate concerning the Jurassic field as none of the Armenian data had been subjected to the complete paleointensity experiment including pTRM checks.

[9] In response, *Tauxe and Yamazaki* [2007] updated the paleointensity database of *Tanaka et al*. [1995] and *Perrin and Schnepp* [2004], using only cooling unit consistency (as recommended by *Thomas and Biggin* [2003]). They recalculated the field averaged over the last 170 Myr to be 63 ZAm^2. They made no comment on the existence of the MDL, however, owing to the paucity of data meeting their minimal acceptance criteria in the Jurassic compared to later time periods.

[10] The problem with estimating a long-term average for the geomagnetic field strength is that it depends not only on the selection criteria applied, but also on the time span over which the average is calculated. Searching the MagIC data base (http://earthref.org/MagIC) for the magic_method_code of LP-PI-TRM (lab protocol-paleointensity-thermal remanence) for data for the last 200 Ma, yields 7054 site means with virtual [axial] dipole moment (V[A]DM) using the directional information associated with the intensity, or a plate tectonic reconstruction (see *Tauxe and Yamazaki* [2007], section 8.2 for details). These are plotted as white triangles in Figure 1 (note that there are five data points in excess of 300 Am^2 that have been left off the plot). Applying the minimum criteria that each data point have a standard deviation of $\leq 15\%$ or ≤ 5 μT, trims the data set down to the 5818 green triangles. Data based on SBG ($N = 389$) are the red dots and those from single crystals ($N = 50$) are blue squares. Median values calculated for 5 Myr bins for bins with at least 10 "reliable" data points (green triangles) are shown as stars. The median value of all the median values is 42 ZAm^2 (shown as the solid cyan line) and the present field value is shown as the dashed magenta line.

[11] There are several striking things about data shown in Figure 1. First, the median value is quite stable with only a few intervals that are much higher than about 60 ZAm^2. Second, and of particular relevance to the present paper, is that there is a prolonged interval with median values consistently lower than 42 ZAm^2 from about 140 Ma to about 180 Ma.

3. Reliability of Submarine Basaltic Glass

[12] In addition to objecting to the criteria used by *Selkin and Tauxe* [2000] for selecting paleointensity data, *Thomas and Biggin* [2003] also objected to their inclusion of results from SBG. The basis for their criticism was the suggestion of *Heller et al*. [2002] that SBG remanences are chemical and not thermal in origin. *Heller et al*. [2002] claimed that because the magnetization of SBG is carried by low-titanium magnetite, which is not an equilibrium phase in mid-ocean ridge basalts (MORBs), it cannot be a primary remanence. However, glass itself is not an equilibrium phase and the equilibrium phase of $Fe_{2.4}Ti_{0.6}O_4$ is not necessarily expected in the glass. On the contrary, iron is more mobile than titanium in the melt and lower titanium magnetites are therefore more likely in the rapidly quenched glass phase [*Zhou et al*., 2000].

[13] *Tauxe and Staudigel* [2004] summarized the evidence that the glassy rinds of submarine pillow

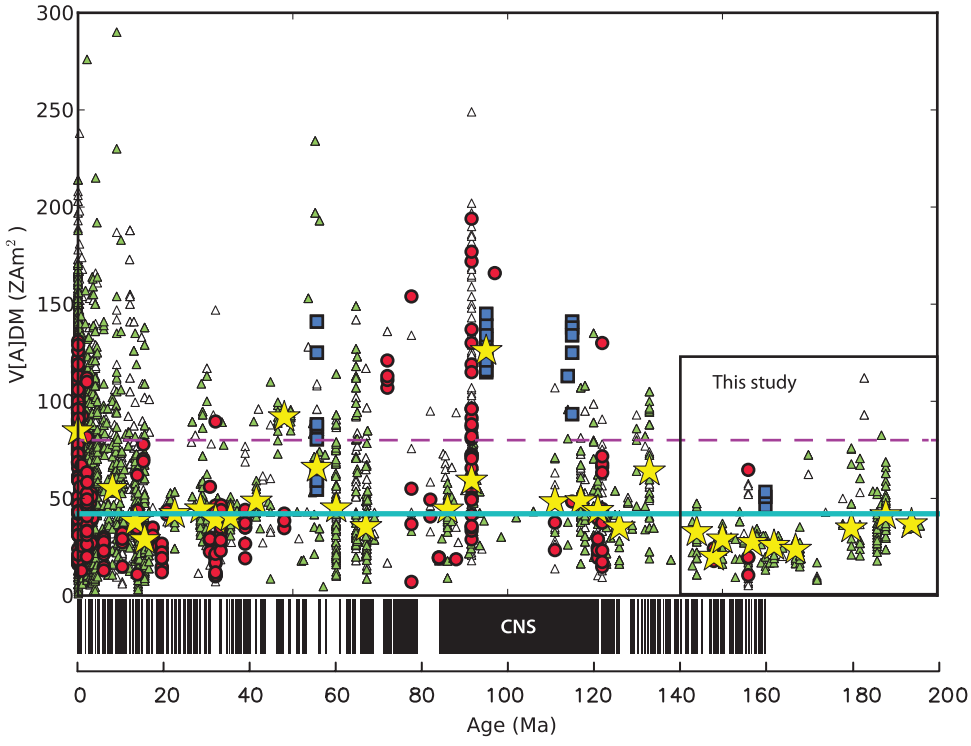

Figure 1. Summary of published data downloaded from the MagIC database. Red dots are submarine basaltic glass data. Blue squares are single crystal results. Triangles are all other data and the light green triangles meet the consistency criteria ($\sigma < 15\%$ of mean or <5 μT); VADMs calculated using the paleolatitudes estimated in *Tauxe and Yamazaki* [2007] for postJurassic data and in this study for the Jurassic data. Magenta dashed line is present field and solid cyan line is long-term stable value for the last 140 Ma. Inset is the time period of interest to the present study.

basalts and sheet flows are excellent materials for paleointensity experiments. While magnetite does grow at elevated temperatures [*Pick and Tauxe*, 1994; *Smirnov and Tarduno*, 2003], the rate of growth drops dramatically below the glass transition temperature [*Bowles et al*., 2011]; hence, the low-Ti magnetite that is present in even zero-age pillow margin glass is likely to have formed during quenching. Paleointensity experiments on basaltic glass from sites of recent eruptions recover the ambient magnetic field at those locations [*Pick and Tauxe*, 1993a, 1993b; *Kent and Gee*, 1996; *Carlut and Kent*, 2000]. Moreover, *Bowles et al*. [2011] succeeded in producing magnetite in experiments that synthesized glass from basaltic melt under various cooling rates and oxygen fugacities. Magnetic data from these experiments are consistent with low-Ti titanomagnetite formed during initial cooling [*Bowles et al*., 2011]. Therefore, the evidence suggests overwhelmingly that the remanence was acquired during quenching, that SBG can evade alteration for geologically significant periods of time and that it frequently behaves in an ideal fashion during the paleointensity experiment. Finally, a study by *Bowles et al*. [2005] shows that by happy coincidence, the cooling rate of submarine basaltic glass during its initial quenching is quite close to the cooling rate of experiments performed in our laboratory. Therefore, there is no rationale for excluding SBG from an analysis of long-term trends in paleointensity.

[14] *Tarduno and Cottrell* [2005] and others have expressed reservations about whole rock paleointensity analyses in general, citing concerns about alteration and advocating the use of the silicate crystals separated from the whole rock as the crystals are armored against alteration. Unlike whole rock analyses on samples of lava flows extruded in known fields, which frequently fail to recover the known field [*Herrero-Bervera and Valet*, 2009], analyses on the plagioclase crystals extracted from the Hawaiian 1955 flow [*Cottrell and Tarduno*, 1999] recovered intensities close to the known field (36.2 μT) almost within error (33.5 $\pm$ 2.4 μT, $N = 5$ specimens).

[15] The twin advantages of single crystals for successful recovery of the known field intensities and a reduced tendency to alter are shared with volcanic glasses. In addition, quenched materials are

more likely to contain the single domain magnetic particles required for a successful paleointensity experiment. *Tauxe* [2006] compiled the existing data from SBG and compared the results with those derived from whole rock data from lava flows for the last 160 Ma. The compilation showed that the intensities from whole rock results are on average higher than those from SBG. *Tauxe* [2006] considered various causes and found that the difference in cooling rate is sufficient to account for the entire difference.

4. Sample Collection and Preparation

[16] There were 57 glass occurrences reported in 400 m of tholeiite [*Plank et al*., 2000] recovered at ODP Hole 801C during Leg 185 (see table available at http://www-odp.tamu.edu/publications/185_IR/chap_03/c3_t5.htm#400763). Glassy materials were examined under a binocular microscope to select glasses with the freshest appearance. Glass chips with magnetic moments larger than 5×10^{-10} A m^2 were wrapped in silica glass fiber, placed in nonmagnetic glass tubes, and fixed with KaSil cement. We prepared a total of 73 specimens from 17 samples and subjected them to a paleointensity experiment.

5. Paleointensity Experiment

[17] The assumptions and various experimental protocols for paleointensity determination are described in detail by *Tauxe and Yamazaki* [2007]. We used the so-called "IZZI" protocol [*Tauxe and Staudigel*, 2004] for the experiments of this study. Briefly, a specimen is heated to some temperature T_i, cooled in zero field and measured. Then, the specimen is heated a second time to the same temperature, cooled in a laboratory field (here 25 μT) and remeasured. This constitutes a "zero-field/infield" or ZI pair. The specimen is then heated to a higher temperature and cooled in the laboratory field, measured and reheated to the same temperature, cooled in zero field, and remeasured. This constitutes an "infield/zero-field" or IZ pair. The IZ steps alternate with the ZI steps, hence the name IZZI for this paleointensty experimental protocol (originally suggested by A. Genevey, personal communication, 2004). After the zero field step in the ZI pairs, we repeat the infield step at the last ZI step to check the ability to acquire partial thermal remanence, a step known as the pTRM check step.

Table 1. Selection Criteria

Specimen Criteria						Sample Criteria	
N_{meas}	β	DANG	FRAC	SCAT	N_{pTRM}	N_{spec}	σ
4	0.1	10	0.5	True	2	2	5 μT

6. Selection Criteria

[18] The IZZI experimental protocol allows us to test many of the fundamental assumptions for paleointensity experiments, such as the presence or absence of alteration during the experiment and the equivalence of thermal blocking and unblocking temperatures. The behavior of specimens during the IZZI experiment is characterized by a number of statistics: the scatter about the slope of the line relating loss of the natural remanence (NRM) to gain of partial thermal remanence (pTRM) in the laboratory, the best-fit line through the directional data, the degree to which pTRM checks agree with the original pTRM, and others [see e.g., *Tauxe et al*., 2010]. The decision on threshold values for the variety of paleointensity parameters has been extremely subjective and is itself the subject of vigorous debate [e.g., *Kissel and Laj*, 2004; *Herrero-Bervera and Valet*, 2009; *Paterson et al*., 2012; *Shaar and Tauxe*, 2013].

[19] The selection criteria used in this study are listed in Table 1. In an effort to reduce the number of statistics and increase the simplicity of the process, *Shaar and Tauxe* [2013] defined two new statistics: SCAT and FRAC. SCAT is meant to replace the various statistics designed to test for sample alteration, pTRM tails and excessive noise in the NRM lost versus pTRM gained (Arai plots of *Nagata et al*. [1963]). The slope of the best-fit line through the data in the Arai plot is allowed to vary within the bounds defined by threshold value of the "scatter" statistic β [*Coe et al*., 1978, renamed by *Selkin and Tauxe*, 2000] which is the ratio of the standard error of the slope σ_b to the absolute value of the slope ($|b|$). The threshold value of β, $\beta_{threshold}$, can be used to define two bounding lines (Figure 2). All NRM, pTRM pairs (including pTRM checks, tail checks and the IZ and ZI pairs) must all fall within the bounding lines for SCAT to be set to "True" (Figure 4). If any point plots outside the bounding lines (see e.g., Figure 3a), SCAT is set to "False." Conversely, if all the points fall within the bounding lines, then SCAT is set as "True." The use of

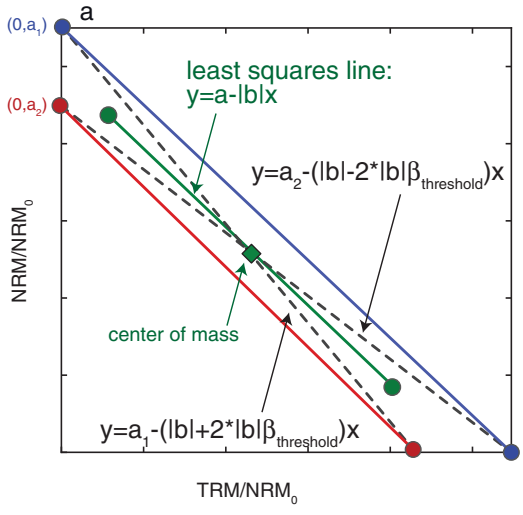

Figure 2. Graphical representations of SCAT definition. SCAT is set to True if all the data points including the pTRM checks and the tail checks fall between the two bounding lines and is False if at least one point falls outside of these bounds. (Figure modified from *Shaar and Tauxe* [2013].)

SCAT obviates the need for complicated strategies for detecting alteration, as long as there are a sufficient number of pTRM check steps within the interval of interest and a sufficiently strict value for $\beta_{threshold}$ is chosen. Here we require at least two check steps and at least four measurement steps (N_{meas}) steps.

[20] FRAC is defined as

$$\mathrm{FRAC} = \frac{\sum_{i=start}^{end-1} |\mathbf{NRM}_{i+1} - \mathbf{NRM}_i|}{VDS},$$

where VDS is the vector difference sum [*Tauxe et al.*, 2010]. FRAC therefore is a measure of the fraction of the total NRM used in the paleointensity calculation. This statistic excludes experiments in which a relatively small proportion of the total NRM contributes to the paleointensity calculation (Figure 3b). Unlike the *f* statistic of *Coe et al.* [1978], which only considers the fraction of a given component, FRAC considers the entire vector difference sum of the remanence. It also corrects a deficiency in the f_{vds} criterion which underestimates the NRM fraction in cases with more scattered data [*Shaar and Tauxe*, 2013].

[21] Setting FRAC to 0.5, instead of closer to unity, allows us to find an interval that passes the FRAC and SCAT test but is associated with a component that does not trend to the origin, hence is not a characteristic direction. To avoid this, we also examine the Deviation ANGle (DANG) [*Tauxe and Staudigel*, 2004] between the selected component and the origin. A value of 10° insures that the component used is the characteristic component; Figure 3c shows an example of a specimen excluded on the basis of DANG.

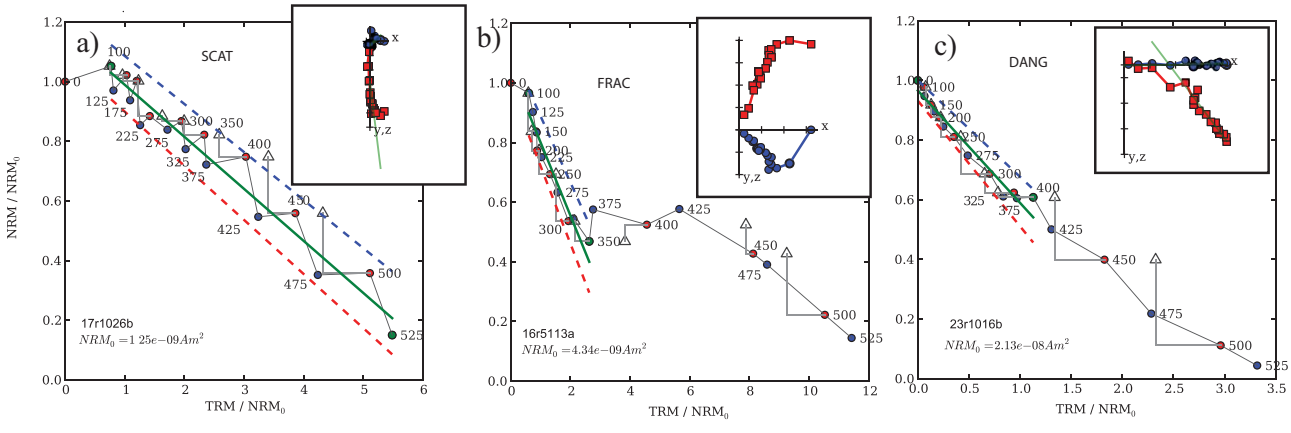

Figure 3. Examples of unsuccessful Thellier experiments plotted as Arai plots [*Nagata et al.*, 1963] with Zijderveld plots [*Zijderveld*, 1967] in the insets. In the Arai plots, red (blue) circles are the ZI (IZ) steps, respectively. The solid green line is the best-fit line within the selected section. Triangles are the repeated infield steps (pTRM checks). In the insets, the blue circles are the *X*, *Y* pairs while the red squares are *X*, *Z* pairs. Note that the samples are unoriented. (a) The zig-zagging nature and poor pTRM checks result in a failed SCAT criterion (there are points outside the SCAT polygon whose boundaries are indicated by the dashed lines. (b) The multicomponent nature of the NRM results in several discrete segments in both the Arai and Zijderveld diagrams. The selected section is too short resulting in a failure of the FRAC criterion. (c) The two component nature of the NRM combined with evident alteration in the higher temperature component means that the low temperature component does not trend to the origin and the specimen fails the DANG criterion.

Table 2. Results by Specimen ODP Hole 801C (Leg 185) SBG Meeting Specimen Criteria in Table 1[a]

Specimen	B (μT)	β	N_{meas}	DANG	T (C)	FRAC
17r1026c	5	0.083	14	10	175–500	0.526
18r2008b	10.2	0.033	13	1.7	0–375	0.573
18r2008e	10.2	0.03	8	2.9	175–350	0.516
22r3014g	16.5	0.044	14	4.2	125–450	0.514
22r3014b	16.7	0.04	9	4.6	250–450	0.513
23r1016a	14.9	0.057	11	4.2	225–475	0.784
23r1016c	17.2	0.025	11	2.4	275–525	0.528
23r1016e	15.5	0.053	11	5.3	100–350	0.523
27r3005b	11.7	0.032	12	8.3	150–425	0.652
28r3043i	7.9	0.048	12	7.4	175–450	0.571
28r3043c	13.7	0.052	10	4.2	225–450	0.53
28r3043a	16.7	0.043	16	6	150–525	0.581
28r3043f	15.7	0.105	5	1.5	375–475	0.519
28r3043d	13.6	0.053	13	8.6	150–450	0.524
28r3043e	13.5	0.05	17	3.8	125–525	0.688
34r2069h	7	0.059	13	9.2	175–475	0.523
34r2069i	11	0.031	14	6.9	200–525	0.533
34r2069j	9	0.065	14	8.6	200–525	0.518
34r2069k	8.6	0.017	18	8.7	100–525	0.824
34r2069l	11.6	0.072	13	9	225–525	0.505
34r2069m	7.8	0.023	14	8.5	175–500	0.587
34r2069c	8.7	0.039	15	3.1	100–450	0.51
34r2069d	8.9	0.029	13	3.8	200–500	0.521
34r2069f	10	0.025	12	5.7	225–500	0.524
34r2069g	7.8	0.045	12	9.3	250–525	0.593
35r3032d	5.2	0.043	16	9.9	125–500	0.764
35r3032f	5.2	0.067	8	8.7	350–525	0.501
35r3032a	10.5	0.049	13	4.3	225–525	0.497
35r3032b	4.1	0.058	11	2.3	250–500	0.581
35r3032c	12.6	0.064	8	4.1	325–500	0.529

[a]Specimen naming scheme is: first three characters (e.g., 35r) are the core, fourth character is the section, characters 5–7 are the sampling horizon (in cm), and the last character is the specimen identifier.

[22] Choosing threshold values for the selection criteria requires a balance between accepting only data of irrefutable quality, of which there may only be a few or none, and having a sufficient number of acceptable results from which to draw inferences about the past field. One key test is the degree of reproducibility at the sample level. One could just use the standard deviation, or standard error of the mean, and if the field values are high (say 100 μT), the standard deviation of the sample mean expressed as a percentage is a useful statistic for screening out samples with poor reproducibility. A requirement of 10%, for example, translates to reproducibility within 10 μT. However, if the field is low (say 10 μT), a standard deviation of say, 10%, would require reproducibility of 1 μT, which is rarely if ever achieved with existing laboratory equipment [*Paterson et al.*, 2012]. For these data, we chose a threshold value of 5 μT for the standard deviation at the sample level; this value is a reasonable one for such low paleointensties as those obtained from these Jurassic basalts.

[23] Having set the specimen level criteria, we find high and low experimental temperature steps for each specimen that result in an interpretation that passes the selection criteria. If more than one set of bounding steps exists that satisfies the selection criteria, the Thellier_GUI program of *Shaar and Tauxe* [2013] chooses the temperature range for each specimen that minimizes the standard deviation at the sample level. A total of 30 specimens (out of the 73 tested) meet the rather strict criteria adopted for this study, a success rate of 41% (Table 2). Specimens failed because of zig-zagging in the Arai plot, or failure to reproduce pTRM values, both of which lead to failure of the SCAT criterion (Figure 3a), or because of multicomponent remanences which led to a failure of the FRAC or DANG criteria (Figures 3b and 3c, respectively). Sample averages from the six acceptable specimens are listed in Table 3. The mean of these six samples is 11.9 ± 3.9 μT. Their locations in the stratigraphic column are plotted as stars in Figure 5. Original measurements and data interpretations for this study have been uploaded into the MagIC database; they can be downloaded from http://earthref.org/MAGIC/9568/ and interpreted using the PmagPy software available from http://earthref.org/PmagPy/cookbook of Tauxe (2010).

7. Paleolatitude of ODP Site 801

[24] The strength of the geomagnetic field is a strong function of latitude; polar intensities are expected to be roughly twice those at the equator. To remove the effect of latitude, it is common practice to convert the field strength values observed into the equivalent dipole moments (Virtual Axial Dipole Moments or VADMs) that would be observed at that (paleo) observation point [*Tauxe et al.*, 2010]. In order to do this, one must have an estimate for the paleolatitude of the observation site.

[25] Paleolatitudes can be estimated in a variety of ways. One can use a global plate reconstruction [e.g., *Besse and Courtillot*, 2002], or the latitude can be calculated from the relationship between average inclination and latitude under the assumption of an axial geocentric dipole. Hole 801C is not on a plate included in global plate reconstructions; therefore, we must rely on paleolatitudes calculated from the inclination data. Inclinations can be determined directly from the paleomagnetic measurement of the basalts recovered from coring, from downhole logging of the drill hole, or from inversion of the seafloor magnetic anomalies near

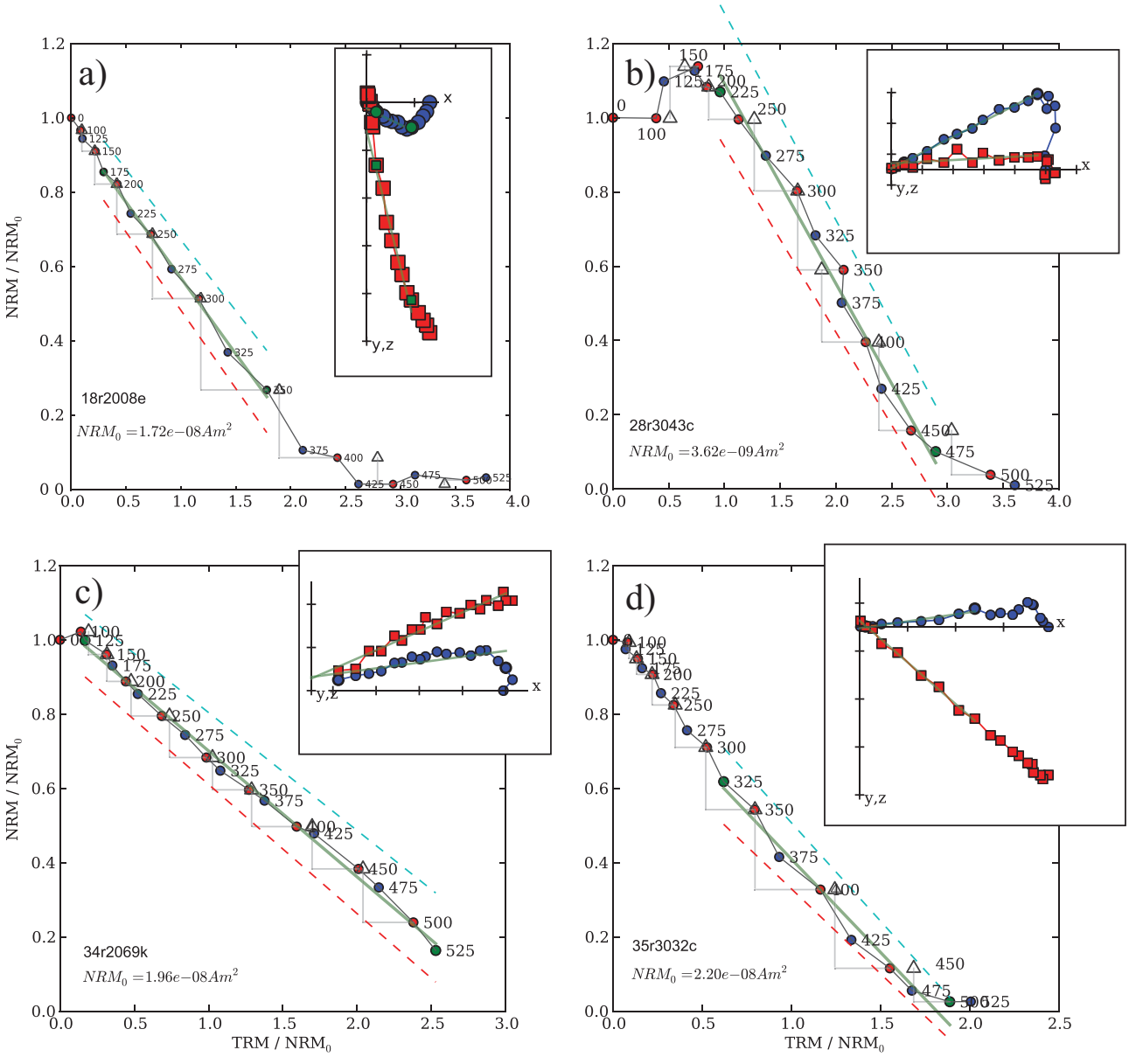

Figure 4. Examples of successful Thellier experiments (see caption to Figure 3 for explanation).

the drill hole. We considered all three lines of evidence.

[26] Paleomagnetic investigations of Hole 801C began during ODP Leg 129 and the results of the basalt measurements were summarized by *Wallick and Steiner* [1992] and *Larson et al.* [1992a] (with a correction of figures in *Larson et al.* [1992b]). Two polarity groups were observed and mean inclinations for this southern hemisphere site were estimated at 27.1° ± 6.9 and −34.8° ± 6.9 for the reverse and normal inclination groups, respectively. The upper part of the hole was logged with a borehole magnetometer during a subsequent leg, ODP Leg 144; *Ito et al.* [1995] estimated apparent inclinations from the downhole logs of approximately 23°. They noted that a significant contribution of viscous or induced magnetization could cause a shallow bias.

[27] Hole 801C was deepened during ODP Leg 185 and magnetic logging results were reported by *Tivey et al.* [2005]. Archive halves were measured at 5 cm intervals and demagnetized in a step-wise fashion using the ship-board magnetometer. Characteristic directions were determined from the shipboard measurements of the archive half in the same fashion as described by *Koppers et al.*

Table 3. Sample Averages of Specimens Listed in Table 2[a]

Sample	Depth (mbsf)	Unit/Subunit	N_{spec}	B (μT)	σ (μT)	VADM (ZAm^2)	1σ
18r2008	643.78	50–10	2	10.2	0	24.3	0
22r3014	676.48	50–40	2	16.6	0.1	39.5	0.3
23r1016	682.06	50–43	3	15.9	1.2	37.8	2.8
28r3043	731.97	50–75	5	13.1	3.2	31.2	7.6
34r2069	787.23	53–3	10	9.0	1.4	21.5	3.4
35r3032	797.94	53–10	4	6.8	3.9	16.2	9.3

[a]Sample name (scheme as in Table 2, but without the specimen identifier). Sample depths are in meters below sea floor based on the coring summary available at: http://www-odp.tamu.edu/publications/185_IR/chap_03/c3_t1.htm#346928. Subunit is the lithological subunit (as opposed to magnetic subunit discussed in the text) as assigned in this table: http://www-odp.tamu.edu/publications/185_IR/VOLUME/TABLES/IR185_03/03_04.TXT. N_{spec} is the number of specimens (in Table 2) that went into the sample mean. B is the average intensity. σ is the standard deviation. σ % is the standard deviation expressed as a percentage of the mean. VADM is the virtual axial dipole moment calculated as described in the text. Average for $B = 11.9\ \mu T \pm 3.9$, VADM $= 28.4 \pm 9.3\ ZAm^2$.

[2012] (but without benefit of core piece lengths to ensure that data ware sufficiently far from piece ends to provide reliable data). These are plotted versus depth in Figure 5. Unit boundaries as described in the lithological logs for ODP Leg 185 are shown as solid lines. Unit 50 (637.23–732.44 mbsf) is exceptionally thick and appears to contain several directional groups in the ship-board inclination data. We have therefore created three "magnetic" subunits within Unit 50, the boundaries of which are shown as dashed lines.

[28] The inclinations inferred from the down-hole magnetic logs [*Tivey et al*., 2005] are in very poor agreement with the data from the archive halves, even at the level of inferred polarity. This and the fact that the downhole logs from Legs 144 and from Leg 185 for the same intervals also disagreed substantially, makes interpretation of the inclination data derived from the logs for the lower portion of the hole difficult. Moreover, there appears to be no systematic shallowing of inclinations downhole in the data from the archive halves, as called for in the progressive tilt model of *Tivey et al*. [2005].

[29] *Larson and Sager* [1992] used the skewness of sea surface magnetic anomalies to estimate a paleolatitude of Site 801 to be ~9°S at 155 Ma or ~3°S if anomalous skewness is taken into account. The bulk of the evidence, therefore, including the magnetic anomaly inversions, point to paleolatitudes of between 3°S and 14°S.

[30] It is clear that there is considerable uncertainty in paleolatitude estimates, which range from 3°S to 27°S. For the purposes of this paper, therefore, we use an estimate of 14°S in order to calculate the Virtual Axial Dipole Moment (VADM). This paleolatitude results in a VADM of $28.1 \pm 8.6\ ZAm^2$. A paleolatitude of 3°S would yield an estimate of 31 ZAm^2 and 20°S would be 26 ZAm^2, so the VADM estimate is not very sensitive to the exact paleolatitude estimate.

8. Discussion

8.1. Independence of the Paleointensity Data From Different Samples

[31] The depths and lithological subunit assignments are given in Table 3 and the locations are plotted in Figure 5. The temporal independence of these samples is not guaranteed as all samples come from just two lithological units (50 and 53). However, Unit 50 comprises at least three directional groupings and it is likely that the Unit 50 paleointensity samples can be considered as independent estimates of field strength. The bottom two are from lithological Unit 53 and it is possible that they registered the same geomagnetic field state.

8.2. Published Jurassic Paleointensity Data

[32] To place the data from Hole 801C into context, we turn to other results published for the Jurassic. The IAGA paleointensity database of *Perrin and Schnepp* [2004] was updated and put into the MagIC database by *Tauxe and Yamazaki* [2007]. That so-called PINT06 compilation included these references for the Jurassic time period: *Kosterov et al*. [1997], *Bol'shakov and Solodovnikov* [1980], *Thomas et al*. [2000], *Bol'shakov and Solodovnikov* [1983], *Briden* [1966], *Tarduno and Cottrell* [2005], *Tauxe* [2006], *van Zijl et al*. [1962], *Bol'shakov et al*. [1987], *Perrin et al*. [1991], and *Sakai and Funaki* [1988]. The most recent update, announced by *Biggin* [2010] and available for download at: http://earth.liv.ac.uk/pint/, added *Shcherbakova et al*. [2009]. In addition to these, *Morales et al*. [2003] has apparently heretofore been overlooked for inclusion in the PINT or MagIC databases.

[33] Of the published data sets, we exclude *Sakai and Funaki* [1988] as these results were based on

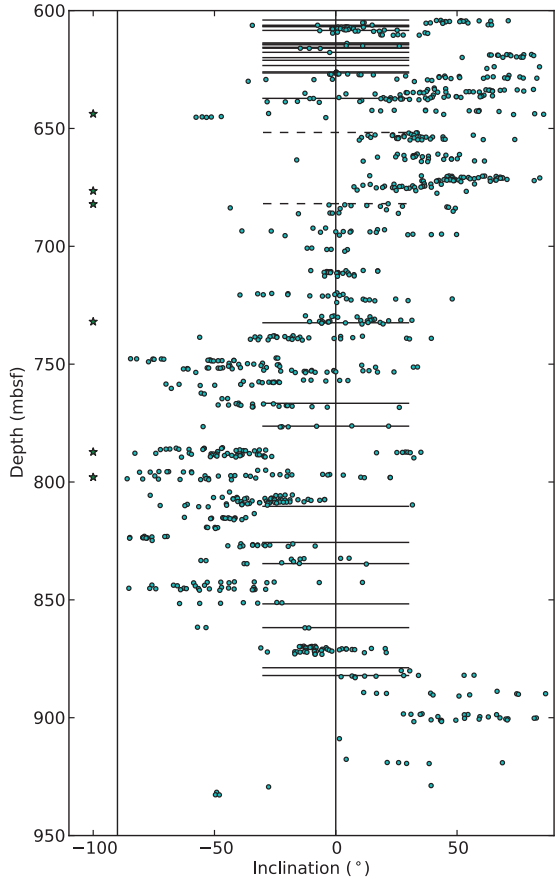

Figure 5. Positions of successful glass samples (stars to left). Inclination data from shipboard (long-core) data as light cyan dots versus meters below sea floor (mbsf). Lithological unit boundaries are shown as solid and additional magnetic unit boundaries as dashed lines, respectively.

thermo-viscous chemical remanence as opposed to a thermal remanence. We also exclude the Gibraltar Microsyenite results of *Thomas et al*. [2000] as these were the low blocking temperature component thought to be a viscous or chemical remanence. The lavas studied by *Derder et al*. [1989] were part of the CAMP igneous province, hence are from the Triassic/Jurassic boundary and are too old. We also exclude the results of *van Zijl et al*. [1962] who noted that the rocks in question had likely been struck by lightning. The remaining Jurassic studies are listed in Table 4. We included the study of *Shcherbakova et al*. [2009] as this has an age range of Tithonian (late Jurassic) to Valanginian (early Cretaceous). We prepared updated MagIC formatted data sets for each of these as follows:

[34] 1. Many errors in the original PINT records were corrected, including missing minus signs in latitudes or longitudes, incorrect units for intensity calculations, incorrect entry of directional data and

Table 4. Table of Published Jurassic Paleointensity Studies From the Magic Database

Location Name	Latitude	Longitude	Age (Ma)		Plate/λ^a	Material	Reference	Age	MagIC Link
Kafan	39	46	152–164	40.5/23.1	EU/33	BC	*Bol'shakov and Solodovnikov* [1983]	*Gradstein et al.* [2004]	9530
Kafan	39	46	136–150	38.9/21.9	EU/21	BC	*Shcherbakova et al.* [2009]	*Gradstein et al.* [2004]	8598
Shampandin	41	45	153–161	54.7/35.3	EU/36	BC	*Bol'shakov and Solodovnikov* [1980]	*Gradstein et al.* [2004]	9536
Karabakh	41	46	167.7 ± 3	45.9/27.3	EU/34	BC	*Bol'shakov et al.* [1987]	*Gradstein et al.* [2004]	9531
North Caucasus	44	42	186 ± 3	48.4/29.2	EU/55	BC	*Bol'shakov et al.* [1987]	*Gradstein et al.* [2004]	9531
169	11	174	148 ± 2		PA/−28	SBG	*Tauxe* [2006]	*Tauxe* [2006]	3474
801B&C	19	156	160.2 ± 0.7		−20	SBG/SC	*Tauxe* [2006] and *Tarduno and Cottrell* [2005] [4,5]	*Koppers et al.* [2003]	3474, 8595
Leg 129									
765	−16	118	155.7 ± 0.3		AU/−36	SBG	*Tauxe* [2006]	*Tauxe* [2006]	3474
Gingenbullen Dolerite	−34	150	172	−80.6/−71.8	AU/−66	Intrusion	*Thomas et al.* [2000]	*Thomas et al.* [2000]	9525
Red Hill	−42	148	185.6 ± 1.5		AU/−61	Intrusion	*Briden* [1966]	*McDougall* [2008]	9532
Granophyre									
Ferrar Dolerite	−75	162	180 ± 3		ANT/−55	Sill	*Briden* [1966]	*Riley and Knight* [2001]	9526
Sani Pass	−30	29	182 ± 2	−49.0/−29.9	AF/−41	Lava flows	*Kosterov et al.* [1997]	*Jourdan et al.* [2007]	9533
Nazareth	−29	28	182 ± 2	−49.0/−29.9	AF/−40	Lava flows	*Kosterov et al.* [1997]	*Jourdan et al.* [2007]	9533
Kerfone	48	355	193	65.9/48.2	EU/36	Dike	*Perrin et al.* [1991]	*Jourdan et al.* [2003]	9534
Tocopilla	−22	290	187	−40.7/−23.3	SA/−24	Lava flows	*Morales et al.* [2003]	*Morales et al.* [2003]	9522

[a] $<I>/\lambda$ is the mean inclination and implied paleolatitude derived from directions in the study. λ: preferred paleolatitude estimate (derived from plate model or other constraint; see text). MAGIC link: go to http://earthref.org/MAGIC/[MagIC link] to retrieve the updated data used in this study. BC: baked contact. SC: single crystal.

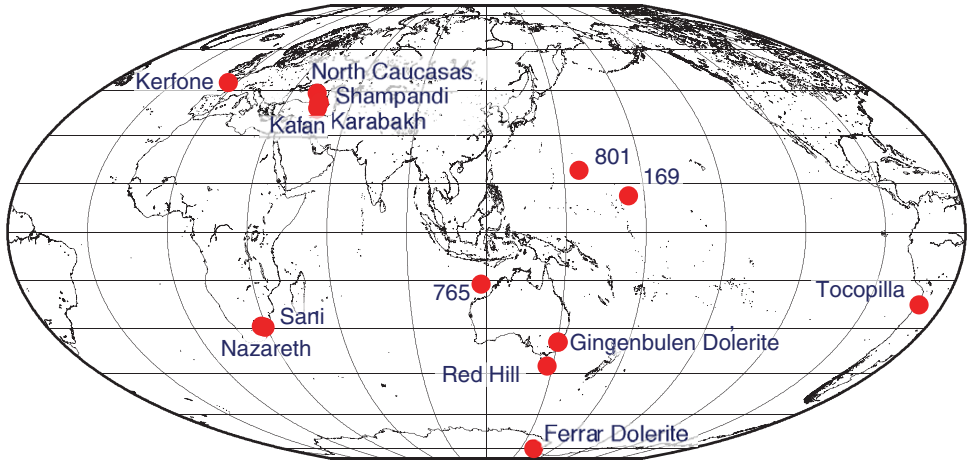

Figure 6. Map of Jurassic sampling locations.

calculations of the Virtual Geomagnetic Pole (VGP) positions, etc.

[35] 2. The method codes, which are essential for searching within the MagIC data model, were checked and enhanced based on information in the papers.

[36] 3. We updated ages as noted in the Age reference column of the table.

[37] The studies of *Bol'shakov and Solodovnikov* [1980, 1983], *Bol'shakov et al*. [1987], and *Shcherbakova et al*. [2009] are on volcanogenic sediments (tuffaceous sandstones and clays) baked by overlying porphyries. These sediments have been mapped as early Jurassic through early Cretaceous with assigned stage names ranging from Pliensbachian to Valanginian. The original references for the geological context are reported in the Russian literature and we do not have access to them. Taking the chronology as reported, we updated the age estimates using the time scale of *Gradstein et al*. [2004]. The ages are likely to be approximately correct to at least the Epoch level (Lower, Middle, Upper Jurassic) or plus or minus 10 Ma. The assigned age uncertainties are at the Stage level here.

[38] The SBG data of *Tauxe* [2006] were all dated based on the anomaly assignment of the basement on which they were drilled. These ages had been determined relative to a recent time scale and are used as is.

[39] All other units were directly dated with radiometric techniques.

[40] 4. We estimated paleolatitudes (λ') for all results (except those for Sites 169 and 801) using the program **apwp.py** in the **PmagPy** software package as described in the PmagPy documentation available here:

[41] http://earthref.org/PmagPy/cookbook

[42] The program **apwp.py** uses the apparent polar wander path for a given plate determined by *Besse and Courtillot* [2002] (listed in Table 4). Also shown in Table 4 are the average inclinations ($<I>$) estimated for the directions as listed in the original studies, if available. As there were frequently both polarities, these were calculated as the directions of the principal components. We converted these average inclinations to equivalent paleolatitudes (λ). In some cases (e.g., Kafan of *Shcherbakova et al*. [2009], Shampandin and Tocopilla), the two paleolatitudinal estimates are in excellent agreement, while others (e.g., North Caucasus, Sani Pass, and Kerfone) are different by more than 10°. We prefer to use the global plate reconstructions, as these are based on the most robust data sets available, while paleolatitudes based on inclinations from a given study may rely on as few as three data points and may also suffer from undocumented structural complications. However, because the paleolatitudes based on global plate reconstructions depend critically on the age estimate, it is possible that poor age control could explain some of the differences (e.g., North Caucasus).

[43] 5. Using the preferred paleolatitudes (λ') listed in Table 4, we (re)calculated VADMs for all results.

[44] All revised data sets were uploaded into the MagIC database and are available using the links listed in Table 4. Figure 6 illustrates the locations of the studies, showing the reasonably global nature of the distribution. The VADMs using the recalculated paleolatitudes (Table 4) and the data

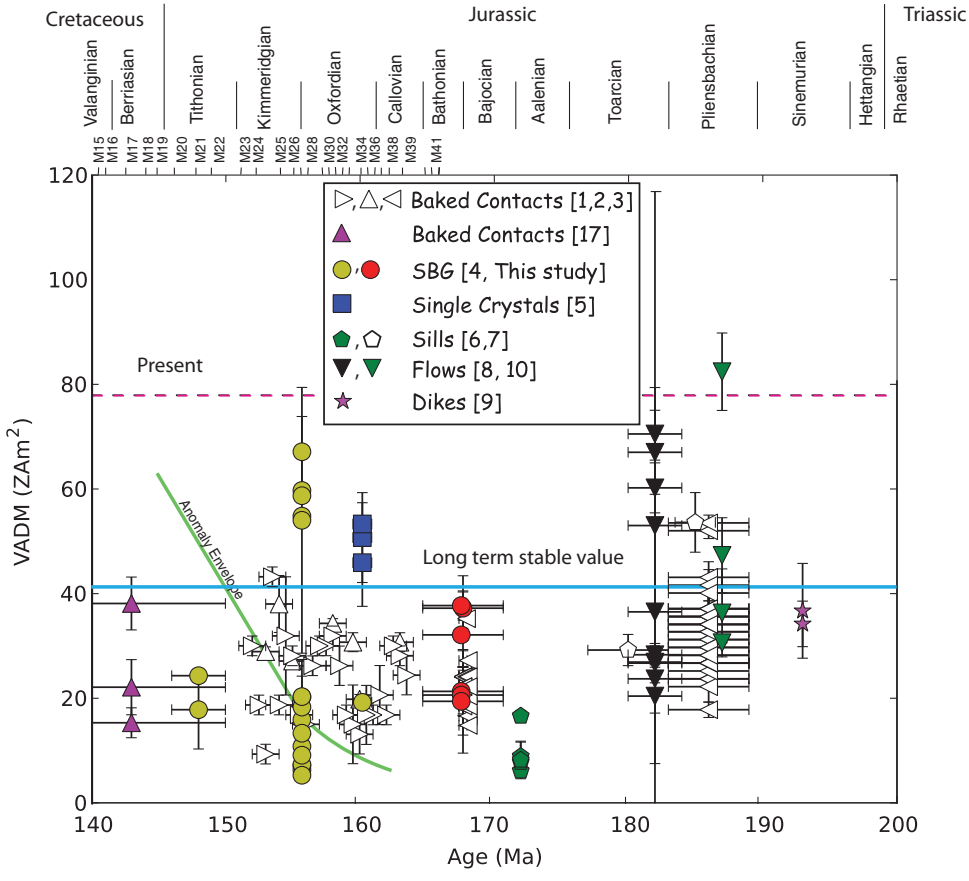

Figure 7. Compilation of Jurassic aged paleointensity data. Long-term stable value (cyan line) is from Figure 1. References as in Table 4. Closed symbols are data points based on Thellier-Thellier method with pTRM checks.

from this study (Table 3) are illustrated in Figure 7. All data are plotted as cooling unit averages, including the new data presented here.

[45] Shown for comparison are the present dipole moment and the median geomagnetic field strength of 42 ZAm^2 for the past 140 Ma estimated from the data in Figure 1. Figure 7 also shows the predicted intensity growth out of the so-called Jurassic Quiet Zone of *McElhinny and Sager* [2003] based on inversions of magnetic anomaly data of *Cande et al*. [1978] and *Sager et al*. [1998]. We have applied no selection criteria apart from excluding results where the authors themselves suspected that the remanence was not a primary TRM. Taken together, the 141 data points from the Jurassic have an average of 28.7 ± 14 ZAm^2.

8.3. Comparison of Different Materials and Methods

[46] Despite the lack of stringent selection criteria, 87% of the 141 cooling unit averages from the entire Jurassic are below the long-term "stable value" of 42 ZAm^2 inferred from Figure 1. This is a remarkable result, in that many of the studies did not include any sort of check for alteration (the open symbols in Figure 7) and only the present study included a test for pTRM tails (a symptom of grain sizes larger than the single domain sizes demanded by the method), as well as a test ensuring that the selected component is the characteristic component, arguably the original TRM. Two of the data points are from a paper published over 40 years ago [*Briden*, 1966]. Nonetheless, the agreement between the SBG results presented here (red dots) with purportedly contemporaneous results from the Armenian baked contacts demonstrates the potential of these baked contacts for paleointensity. Moreover, the overwhelming majority of the results strongly support the contention that the geomagnetic field was much lower than the long-term stable value estimated for the last 140 Myr.

8.4. Duration of the Mesozoic Dipole Low

[47] That the field was generally low during the Jurassic is apparent from the compilation of data

shown in Figures 1 and 7. However, the bounds of this Mesozoic Dipole Low are not well constrained. The data from the CAMP units studied by *Derder et al*. [1989] are ~196–201 Ma [*Marzoli et al*., 2011] and have quite high VADM values of ~100 ZAm^2. This may suggest that the lower boundary of the MDL is in the early Jurassic, perhaps after the eruption of the Lesotho Basalt (Sani Pass and Nazareth in Table 4) investigated by *Kosterov et al*. [1997] and dated at 182 ± 2 Ma by *Jourdan et al*. [2007].

[48] The study of *Bol'shakov and Solodovnikov* [1983] presents baked contact data from the period 134–140 Ma (early Cretaceous) which have similar values to those shown in Figure 7 so the MDL could extend into the early Cretaceous. However, *Goguitchaitchvili et al*. [2002b] published data from the Paraná flood basalt sequence (dated at 132–133 Ma by *Renne et al*. [1996]) and found VADMs ranging from 40 to over 100 ZAm^2 with an average of about 72 ZAm^2 or very nearly the present day value. So the MDL may have started in the early Jurassic (~182 Ma) and ended before 133 Ma.

[49] The nearly 50 Myr duration of the Mesozoic Dipole Low supported by the data compiled here contrasts with the rather short duration called for by, e.g., *Tarduno and Cottrell* [2005], who sought to tie average reversal frequency with average field strength. It is worth pointing out that *Tauxe and Yamazaki* [2007] took a slightly different approach by tying average field strength within an individual polarity interval with the duration of that interval. This is more difficult to do because it is rare to be able to tie a particular result with a given polarity interval owing to the short duration of most polarity intervals and the large uncertainties in ages. Nonetheless, the six intervals that they found suggested a relationship between average VADM with the log of the polarity interval length. Short polarity intervals (less than 1 Ma) had average VADMs of 41 ± 26 ZAm^2 ($N = 35$). Data from C26r, which has a duration of about 3 Myr, had an average VADM of 55 ± 16 ZAm^2 ($N = 6$). The data from the Cretaceous Normal Superchron (spanning from 121 to 84 Ma or ~37 Myr) had an average of 89 ± 48 ZAm^2 ($N = 43$). According to the analysis of *Tauxe and Yamazaki* [2007], then, polarity intervals would need to be longer than about one million years to have average values higher than the long-term stable value and this duration is quite rare in the early Cretaceous and Jurassic, although the geomagnetic reversal time scale is poorly constrained prior to about 170 Ma. The approach taken here of plotting median values of five million year intervals, as done in Figure 1, however, is less influenced by extreme outliers and does not strongly support the notion of a very high field average value during the CNS. Apart for a brief interval represented by the single crystal data of *Tarduno and Cottrell* [2005], the median values throughout the CNS are indistinguishable from the data observed since. So according to this reanalysis, there is no strong connection between reversal frequency and median field strength. Moreover, if the high quality paleointensity data from *Shcherbakova et al*. [2009] (purple triangles in Figure 7) have robust ages, then the MDL extended well beyond the rise in the anomaly envelope of *Cande et al*. [1978] (green line in Figure 7), which reached the long-term stable value by about 150 Ma.

[50] When attempting to attribute the reduction in VADM to a geodynamic driver, it is interesting to note that *Kent and Irving* [2010] recently called for a "monster shift" (the 1J shift) in the apparent polar wander path of Pangea between about 160 Ma and 140 Ma. The termination of the 1J shift at about 140 Ma coincides with the termination of the MDL, but the onset at 160 Ma occurs within the middle of the MDL. Thus, it seems unlikely that there is a connection between these two phenomena although better ages and more paleointensity data could strengthen the relationship.

9. Conclusions

[51] Nearly all of the results from Jurassic aged rocks suggest field values that are lower than the stable field value for the last 140 Myr of ~42 ZAm^2. The Jurassic average 28.1 ± 8.6 ZAm^2 is ~35% of the present field value and 66% of the long-term value. A low Jurassic field is supported by data from all over the world, from a variety of rock types and experimental designs and without regard to objective measures of quality. In particular, results from submarine basaltic glass utilizing the most robust experimental design to date are replicated by results from other contemporaneous recording media. We have now addressed concerns about the provincial nature of Jurassic data sets, reliance on a single rock type and lack of data that pass strict selection criteria. The existence of a long-lived Mesozoic Dipole Low is supported. It likely began in the earliest Jurassic and endured

throughout the Jurassic and into the Cretaceous. The field returned to higher field values by about 133 Ma. If the data for the late Jurassic and early Cretaceous are correct, then the low field extended well beyond the increase in reversal frequency at around M19 time.

Acknowledgments

[52] We acknowledge Jason L. Steindorf for careful laboratory measurements. This material is based upon work supported by the National Science Foundation under grants EAR 0126561 to M.S. and OCE1058858 and EAR1141840 to L.T. The manuscript greatly benefited from careful and constructive reviews by one anonymous reviewer, Mirielle Perrin, and the Associate Editor, Sue Beske-Diehl.

References

Besse, J., and V. Courtillot (2002), Apparent and true polar wander and the geometry of the geomagnetic field over the last 200 Myr, *J. Geophys. Res.*, *107*(B11), 2300, doi:10.1029/2000JB000050.

Biggin, A. (2010), Paleointensity database updated and upgraded, *Eos Trans. AGU*, *91*, 15.

Biggin, A., B. Steinberger, J. Aubert, N. Suttie, R. Holme, T. H. Torsvik, D. van der Meer, and D. van Hinsbergen (2012), Possible links between long-term geomagnetic variations and whole-mantle convection processes, *Nat. Geosci.*, *5*, 526–533.

Biggin, A. J., and D. N. Thomas (2003), Analysis of long-term variations in the geomagnetic poloidal field intensity and evaluation of their relationship with global geodynamics, *Geophys. J. Int.*, *152*, 392–415.

Bol'shakov, A., and G. M. Solodovnikov (1980), Paleomagnetic data on the intensity of the magnetic field of the Earth, *Izv. Earth Phys.*, *16*, 602–614.

Bol'shakov, A., and G. M. Solodovnikov (1983), Geomagnetic field intensity in Armenia in the Late Jurassic and Early Cretaceous, *Izv. Earth Phys.*, *19*, 976–982.

Bol'shakov, A., G. M. Solodovnikov, and Y. K. Vinogradov (1987), Paleointensity of the geomagnetic field in the Middle Jurassic, *Izv. Earth Phys.*, *23*, 324–333.

Bowles, J., J. S. Gee, D. Kent, E. Bergmanis, and J. Sinton (2005), Cooling rate effects on paleointensity estimates in submarine basaltic glass and implications for dating young flows, *Geochem. Geophys. Geosyst.*, *6*, Q07002, doi:10.1029/2004GC000900.

Bowles, J., J. S. Gee, K. Burgess, and R. Cooper (2011), Timing of magnetite formation in basaltic glass: Insights from synthetic analogs and relevance for geomagnetic paleointensity analysis, *Geochem. Geophys. Geosyst.*, *12*, Q02001, doi:10.1029/2010GC003404.

Briden, J. C. (1996), Variation of intensity of the palaeomagnetic field through geologic time, *Nature*, *212*, 246–247.

Cande, S., R. Larson, and J. LaBrecque (1978), Magnetic lineations in the Pacific Jurassic Quiet zone, *Earth Planet. Sci. Lett.*, *41*, 434–440.

Carlut, J., and D. Kent (2000), Paleointensity record in zero-age submarine basalt glass: Testing a new dating technique for recent MORBS, *Earth Planet. Sci. Lett.*, *183*, 389–401.

Coe, R. S., S. Grommé, and E. A. Mankinen (1978), Geomagnetic paleointensities from radiocarbon-dated lava flows on Hawaii and the question of the Pacific nondipole low, *J. Geophys. Res.*, *83*, 1740–1756.

Cottrell, R., and J. Tarduno (1999), Geomagnetic paleointensity derived from single plagioclase crystals, *Earth Planet. Sci. Lett.*, *169*, 1–5.

Courtillot, V., and J. Besse (1987), Magnetic field reversals, polar wander, and core-mantle coupling, *Science*, *237*, 1140–1147.

Derder, M. E. M., J. Thompson, M. Prévot, and M. McWilliams (1989), Geomagnetic field intensity in Early Jurassic: Investigation of the Newark Supergroup (eastern North America), *Phys. Earth Planet. Inter.*, *58*, 126–136.

Goguitchaitchvili, A., J. Urrutia-Fucugauchi, and L. Alva-Valdivia (2002a), Mesozoic Dipole Low: Myth or reality?, *Eos Trans. AGU*, *83*, 457.

Goguitchaitchvili, A., L. Alva-Valdivia, J. Urrutia-Fucugauchi, and J. Morales (2002b), On the reliability of Mesozoic Dipole Low: New absolute paleointensity results from Paranaá Flood Basalts (Brazil), *Geophys. Res. Lett.*, *29*(12), 33-1–33-4, doi:10.1029/2002GL015242.

Gradstein, F., J. Ogg, and A. Smith (2004), *Geologic Time Scale 2004*, Cambridge Univ. Press, Cambridge, U. K.

Heller, R., R. T. Merrill, and P. L. McFadden (2002), The variation of intensity of earth's magnetic field with time, *Phys. Earth Planet. Inter.*, *131*, 237–249.

Helsley, C., and M. Steiner (1969), Evidence for long intervals of normal polarity during the Cretaceous period, *Earth Planet. Sci. Lett.*, *5*, 325–332.

Herrero-Bervera, E., and J. P. Valet (2009), Testing determinations of absolute paleointensity from the 1955 and 1960 Hawaiian flows, *Earth Planet. Sci. Lett.*, *287*, 420–433.

Ito, H., Y. Nogi, and R. Larson (1995), Magnetic reversal stratigraphy of Jurassic oceanic crust from Hole 801C downhole magnetometer measurements, *Proc. Integrated Ocean Drill. Program Sci. Results*, *144*, 641–647.

Jourdan, F., A. Marzoli, H. Bertram, M. Cosca, and D. Fontignie (2003), The northernmost CAMP: Ar/Ar age, petrology and Sr-Nd-Pb isotope geochemistry of the Kerforne dyke, Brittany, France in *The Central Atalantic Magmatic Province*, W. Hames, J. G. McHone, C. Rupel, P. R. Renne, ed., 136, 209–226, AGU Monograph, American Geophysical Union, Washington, D. C.

Jourdan, F., G. Féraud, H. Bertrand, M. Watkeys, and P. Renne (2007), Distinct brief major events in the Karoo large igneous province clarified by new $^{40}Ar/^{39}Ar$ ages on the Lesotho basalts, *Lithos*, *98*, 195–209.

Juarez, T., L. Tauxe, J. S. Gee, and T. Pick (1998), The intensity of the Earth's magnetic field over the past 160 million years, *Nature*, *394*, 878–881.

Kent, D., and E. Irving (2010), Influence of inclination error in sedimentary rocks on the Triassic and Jurassic apparent pole wander path for North America and implications for Cordilleran tectonics, *J. Geophy. Res.*, *115*, B10103, doi:10.1029/2009JB007205.

Kent, D. V., and J. Gee (1996), Magnetic alteration of zero-age oceanic basalt, *Geology*, *24*, 703–706.

Kissel, C., and C. Laj (2004), Improvements in procedure and paleointensity selection criteria (PICRIT-03) for Thellier and Thellier determinations: Application to Hawaiian basaltic long cores, *Phys. Earth Planet. Inter.*, *147*, 155–169.

Koppers, A., H. Staudigel, and R. Duncan (2003), High-resolution $^{40}Ar/^{39}Ar$ dating of the oldest oceanic basement

basalts in the western Pacific basin, *Geochem. Geophys. Geosyst.*, *4*(11), 8914, doi:10.1029/2003GC000574.

Koppers, A., T. Yamazaki, J. Geldmacher, J. S. Gee, N. Pressling, H. Hoshi, and S. Party (2012), Limited latitudinal mantle plume motion for the Louisville hotspot, *Nat. Geosci.*, *5*, 911–917.

Kosterov, A., M. Prevot, M. Perrin, and V. Shashkanov (1997), Paleointensity of the Earth's magnetic field in Jurassic: New results from a Thellier study of the Lesotho Basalt, southern Africa, *J. Geophys. Res.*, *102*, 24,859–24,872.

Larson, R., and W. Sager (1992), *Skewness of Magnetic Anomalies M0 to M29 in the Northwestern Pacific*, vol. *129*, pp. 471–481, Ocean Drill. Program, College Station, Tex.

Larson, R., M. Steiner, E. Erba, and Y. Lancelot (1992a), Paleolatitudes and tectonic reconstructions of the oldest portion of the Pacific Plate: A comparative study *129*, 615–631.

Larson, R., M. Steiner, E. Erba, and Y. Lancelot (1992b), Corrections to Paleolatitudes and tectonic reconstructions of the oldest portion of the Pacific Plate: A comparative study, *Proc. Ocean Drill. Program Sci. Results*, *129*, 618–619.

Marzoli, A., et al. (2011), Timing and duration of the Central Atlantic magmatic province in the Newark and Culpeper basins, eastern U.S.A., *Lithos*, *122*, 175–188.

McDougall, I. (2008), Geochronology and the evolution of Australia in the Mesozoic, *Aust. J. Earth Sci.*, *55*, 849–864.

McElhinny, M., and W. Sager (2003), Jurassic dipole low defined from land and sea data, *Eos Trans. AGU*, *84*, 362.

McFadden, P. L., and M. W. McElhinny (1982), Variations in the geomagnetic dipole 2: Statistical analysis of VDM's for the past 5 m.y., *J. Geomagn. Geoelctr.*, *34*, 163–189.

Morales, J., A. Goguitchaitchvili, L. Alva-Valdivia, and J. Urrutia-Fucugauchi (2003), Absolute paleointensity of the Earth's magnetic field during Jurassic: Case study of La Negra Formation (northern Chile), *C. R. Geosci.*, *335*, 661–670.

Nagata, T., Y. Arai, and K. Momose (1963), Secular variation of the geomagnetic total force during the last 5000 years, *J. Geophys. Res.*, *68*, 5277–5282.

Paterson, G., A. Biggin, Y. Yamamoto, and Y. X. Pan (2012), Towards the robust selection of Thellier-type paleointensity data: The influence of experimental noise, *Geochem. Geophys. Geosyst.*, *13*, Q05Z43, doi:10.1029/2012GC004046.

Perrin, E. A., M. Prevot, and M. Mankinen (1991), Low intensity of the geomagnetic field in early Jurassic Time, *J. Geophys. Res.*, *96*, 14,197–14,210.

Perrin, M., and E. Schnepp (2004), IAGA paleointensity database: Distribution and quality of the data set, *Phys. Earth Planet. Inter.*, *147*, 255–267.

Perrin, M., and V. Shcherbakov (1997), Paleointensity of the Earth's magnetic field for the past 400 Ma: Evidence for a dipole structure during the Mesozoic low, *J. Geomagn. Geoelectr.*, *49*(4), 601–614.

Pick, T., and L. Tauxe (1993a), Geomagnetic paleointensities during the Cretaceous normal superchron measured using submarine basaltic glass, *Nature*, *366*, 238–242.

Pick, T., and L. Tauxe (1993b), Holocene paleointensities: Thellier experiments on submarine basaltic glass from the East Pacific Rise, *J. Geophys. Res.*, *98*, 17,949–17,964.

Pick, T., and L. Tauxe (1994), Characteristics of magnetite in submarine basaltic glass, *Geophys. J. Int.*, *119*, 116–128.

Plank, T., J. Ludden, and C. Escutia (2000), Initial Reports, *Proc. Ocean Drill. Program Initial Rep.*, *185*

Prévot, M., M. E. M. Derder, M. McWilliams, and J. Thompson (1990), Intensity of the Earth's magnetic field: Evidence for a Mesozoic Dipole Low, *Earth Planet. Sci. Lett.*, *97*, 129–139.

Renne, P. R., K. Deckart, M. Ernesto, G. Feraud, and E. M. Piccirillo (1996), Age of the Ponta Grossa dike swarm (Brazil), and implications to Paraná flood volcanism, *Earth Planet. Sci. Lett.*, *144*, 199–211.

Riley, T., and K. Knight (2001), Age of pre-break-up Gondwana magmatism: A review, *Antarct. Sci.*, *13*, 99–110.

Sager, W., C. Weiss, M. Tivey, and H. Johnson (1998), Geomagnetic polarity reversal model of deep-tow profiles from the Pacific Jurassic Quiet Zone, *J. Geophys. Res.*, *103*, 5269–5286.

Sakai, H., and M. Funaki (1988), Paleomagnetic study of the Beacon Supergroup in Antarctica: Remagnetization in the Jurassic Time, *Proc. NIPR Symp. Antarct. Geosci.*, *2*, 46–54.

Selkin, P., and L. Tauxe (2000), Long-term variations in paleointensity, *Philos. Trans. R. Soc. London A*, *358*, 1065–1088.

Shaar, R., and L. Tauxe (2013), Thellier_GUI: An integrated tool for analyzing paleointensity data from Thellier-type experiments, *Geochem. Geophys. Geosyst.*, *14*, 677–692, doi:10.1002/ggge.20062.

Shcherbakova, V., M. Perrin, V. Shcherbakov, V. Pavlov, A. Ayvaz'yan, and G. Zhidkov (2009), Rock magnetic and paleointensity results from Mesozoic baked contacts of Armenia, *Earth Planets Space*, *61*, 23–39.

Smirnov, A. V., and J. A. Tarduno (2003), Magnetic hysteresis monitoring of Cretaceous submarine basaltic glass during Thellier paleointensity experiments: Evidence for alteration and attendant low field bias, *Earth Planet. Sci. Lett.*, *206*, 571–585.

Tanaka, H., M. Kono, and H. Uchimura (1995), Some global features of paleointensity in geological time, *Geophys. J. Int.*, *120*, 97–102.

Tarduno, J. A., and R. D. Cottrell (2005), Dipole strength and variation of the time-averaged reversing and nonreversing geodynamo based on Thellier analyses of single plagioclase crystals, *J. Geophys. Res.*, *110*, B11101, doi:10.1029JB 003970.

Tarduno, J. A., and J. Gee (1995), Large-scale motion between Pacific and Atlantic hotspots, *Nature*, *378*, 477–480.

Tarduno, J. A., and A. V. Smirnov (2001), Stability of the Earth with respect to the spin axis for the last 130 million years, *Earth Planet. Sci. Lett.*, *184*, 549–553.

Tauxe, L. (2006), Long-term trends in paleointensity: The contribution of DSDP/ODP submarine basaltic glass collections, *Phys. Earth Planet. Inter.*, *156*, 223–241.

Tauxe, L., and H. Staudigel (2004), Strength of the geomagnetic field in the Cretaceous Normal Superchron: New data from submarine basaltic glass of the Troodos Ophiolite, *Geochem. Geophys. Geosyst.*, *5*, Q02H06, doi:10.1029/2003GC000635.

Tauxe, L., and T. Yamazaki (2007), Paleointensities, in Geomagnetism, *Treatise on Geophysics*, vol. *5*, edited by M. Kono, pp. 509–563, Elsevier, Amsterdam.

Tauxe, L., S. K. Banerjee, R. Butler, and R. van der Voo (2010), *Essentials of Paleomagnetism*, Univ. of Calif. Press, Berkeley.

Thomas, D., A. Biggin, and P. Schmidt (2000), A paleomagnetic study of Jurassic intrusives from southern New Sourth

Wales: Further evidence for a pre-Cenozoic dipole low, *Geophys. J. Int.*, *140*, 621–635.

Thomas, D. N., and A. Biggin (2003), Does the Mesozoic Dipole Low really exist, *Eos Trans. AGU*, *84*(97), 103.

Tivey, M., R. Larson, H. Schouten, and R. Pockalny (2005), Downhole magnetic measurements of ODP Hole 801C: Implications for Pacific oceanic crust and magnetic field behavior in the Middle Jurassic, *Geochem. Geophys. Geosyst.*, *6*, Q04008, doi:10.1029/2004GC000754.

van Zijl, J., K. Graham, and A. Hales (1962), The paleomagnetism of the Stormberg Lavas, 2. The behavior of the Earth's magnetic field during a reversal, *Geophys. J. R. Astron. Soc.*, *7*, 169–182.

Wallick, B., and M. B. Steiner (1992), *Paleomagnetism of Cretaceous basalts from the East Mariana Basin, Western Pacific Ocean*, pp. 447–454, Ocean Drill. Program, College Station, Tex.

Zhou, W., R. van der Voo, D. Peacor, and Y. Zhang (2000), Variable Ti-content and grain size of titanomagnetite as a function of cooling rate in very young MORB, *Earth Planet. Sci. Lett.*, *179*, 9–20.

Zijderveld, J. D. A. (1967), A.C. demagnetization of rocks: Analysis of results, in *Methods in Paleomagnetism*, Chapman and Hall. edited by D. Collinson, pp. 254–286, London.